University of Wollongong

Research Online

2017

Kinetic study of thermal degradation of chitosan as a function of deacetylation degree

M A. Gámiz-González
Polytechnical University of Valencia

Daniela M. Correia
University of Minho

Senentxu Lanceros-Mendez
University of Minho

Vitor Sencadas
University of Wollongong, victors@uow.edu.au

J L. Gomez Ribelles
Universidad Politecnica de Valencia

See next page for additional authors

Follow this and additional works at: https://ro.uow.edu.au/eispapers1

Part of the Engineering Commons, and the Science and Technology Studies Commons

Recommended Citation

Kinetic study of thermal degradation of chitosan as a function of deacetylation degree

Abstract

Thermal degradation of chitosan with varying deacetylation degree (DD) ranging between 50 and 85% was analyzed by dynamic thermogravimetric analysis at different heating rates. The present study focused on the temperature range between 500 and 800 K, above water evaporation. Thermal degradation showed a main degradation stage in this temperature interval with a second stage that appeared in the weight derivative curves as a shoulder in the high temperature side of the main peak with increasing intensity as the DD decreased. The Kissinger and isoconversional Ozawa-Flynn-Wall models were employed to evaluate the Ea of both thermal degradation processes. Different kinetic models were tested to computer simulate the thermogravimetric traces calculating the model parameters with a non-linear least squares fitting routine. The Sestack-Berggren model allowed reproducing accurately the overlapping of the two degradation mechanisms and calculating the mass fraction lost in each of them revealing the coupling between the two degradation mechanisms.

Disciplines

Engineering | Science and Technology Studies

Publication Details

Authors

M A. Gámiz-González, Daniela M. Correia, Senentxu Lanceros-Mendez, Vitor Sencadas, J L. Gomez Ribelles, and A Vidaurre

Kinetic study of thermal degradation of chitosan as a function of deacetylation degree.

M. A. Gámiz-González [a*], D. M. Correia [b,c], S. Lanceros-Mendez [c,d,e], V. Sencadas [f], J. L. Gómez Ribelles [a,g] and A. Vidaurre [a,g].

[a] *Centre for Biomaterials and Tissue Engineering (CBIT), Universitat Politècnica de València, Cno. de Vera s/n, 46022 Valencia, Spain.*

[b] *Centro de Quımica, Universidade do Minho, Campus de Gualtar, 4710-057 Braga, Portugal*

[c] *Centro de Fisica, Universidade do Minho, Campus de Gualtar, 4710-058 Braga, Portugal*

[d] *BCMaterials, Basque Center for Materials, Applications and Nanostructures, Parque Tecnologico de Bizkaia, 48160 Derio, Spain*

[e] *IKERBASQUE, Basque Foundation for Science, 48013 Bilbao, Spain*

[d] School of Mechanical, Materials and Mechatronics Engineering, University of Wollongong, Wollongong NSW 2522, Australia.

[e] *Biomedical Research Networking Center on Bioengineering, Biomaterials and Nanomedicine (CIBER-BBN), Valencia, Spain*

Abstract

Thermal degradation of chitosan with varying deacetylation degree (DD) ranging between 50 and 85% was analyzed by dynamic thermogravimetric analysis at different heating rates. The present study focused on the temperature range between 500 and 800 K, above water evaporation. Thermal degradation showed a main degradation stage in this temperature interval with a second stage that appeared in the weight derivative curves as a shoulder in the high temperature side of the main peak with increasing intensity as the DD decreased. The Kissinger and isoconversional Ozawa-Flynn-Wall models were employed to evaluate the E_a of both thermal degradation processes. Different kinetic models were tested to computer simulate the thermogravimetric traces calculating the model parameters with a non-linear least squares fitting routine. The Sestack-Berggren model allowed reproducing accurately the overlapping of the two

degradation mechanisms and calculating the mass fraction lost in each of them revealing the coupling between the two degradation mechanisms

Highlights

Coupling of the degradation of acetylated and deacetilated units in chitosan with varying deacetylation degree.

Model fitting of degradation in overlapped degradation mechanisms.

Previous activation energy determination by applying "free model" methods allows subsequent model fitting of TGA traces.

Sestack-Berggren model yields the best fit to the experimental data in chitosan.

Keywords

Chitosan, deacetylation degree, thermal degradation, thermogravimetric analysis, kinetic models, activation energy.

1.Introduction

Chitin is a polysaccharide composed of N-acetyl-D-Glucosamine groups linked by O-glucosidic bonds β(1→4). It is the second most abundant polysaccharide in nature and it is obtained from natural sources such as shrimp and crab shells. The alkaline deacetylation process of chitin promotes its conversion to chitosan formed by N-Acetyl-D-glucosamine and D-Glucosamine units (Lim & Hudson, 2003), chitosan has good properties as a biopolymer and is widely used in fields such as the food industry, pharmacy and medicine (Muzzarelli, 2009), (Peluso et al., 1994)

The deacetylation degree (DD) of chitosan determines the ratio between D-glucosamine and N-acetyl -D -glucosamine units in the polymer chains. DD over 50% is considered to be chitosan and below 50 % the polymer is called chitin (Pillai, Paul, & Sharma, 2009). The properties of the polymer are strongly dependent on the DD.

Chitosan with varying DD can be obtained by acetylation of high DD chitosan, the reaction yield being controlled by the concentration of acetic anhydride solution added in the reaction (Hirano, Ohe, & Ono, 1976) (Hirano et al., 1976).

The thermal degradation of chitin and chitosan has been previously studied by thermogravimetric analysis, TGA, by different authors. The main weight loss stage measured in heating scans in nitrogen atmosphere appears at higher temperatures in chitin than in chitosan, the difference between then being around 340 k (Wanjun, Cunxin, & Donghua, 2005). In the case of chitosan with varying DD the thermogram shows traces of a second degradation stage in the range of temperatures of the main degradation process of chitin(Nam, Park, Ihm, & Hudson, 2010; Nieto, Peniche-Covas, & Padro, 1991). Thermal degradation of both polymers occurs by the cleavage of glycosidic linkages (C-O-C) (Wanjun, Cunxin, & Donghua, 2005).

Nevertheless, the fact that the weight loss in chitin shift towards higher temperatures in TGA scans with respect to chitosan supports a change in the kinetics of bond cleavage with the presence of acetylated groups.

The aim of this work is to analyze coupling between the two degradation stages in chitosan with varying DD. We are going to show that the experimental thermograms are not merely a superposition of the processes due to acetylated and deacetylated groups. This analysis requires characterizing the kinetics of

degradation. In a first step the activation energy will be determined with equations independent of any kinetic model. The values obtained for the main degradation stage were used to select the best kinetic model for this particular co-polymer following a non-linear least squares fitting routine to the experimental TGA traces. Nevertheless, this model shows inconsistent values in the case of the weaker process when two degradation mechanisms superpose. Once the kinetic model is applied, simultaneously to both degradation processes the strength of each weight loss stage is determined, allowing reaching conclusions on the coupling of the overlapped degradation processes

1.1 General form of the kinetic model

The kinetics of the thermal degradation process can be evaluated from the thermogravimetric data, considering that the degradation rate only depends on two variables, temperature, T and conversion degree, α (Vyazovkin et al., 2011):

$$\frac{d\alpha(t)}{dt} = k(T)f[\alpha(t)] \tag{1}$$

The degree of conversion is defined by:

$$\alpha = \frac{w_0 - w_{(t)}}{w_0 - w_\infty} \tag{2}$$

w_0, $w_{(t)}$, and w_∞, being the weights of the sample before degradation, at a given time t and after complete degradation, respectively. The value of α reflects the progress of the overall transformation that can involve multiple steps, each of which has its specific extent of conversion and f(α) is the kinetic reaction model.

The temperature dependence of the degradation rate is usually parametrized through the Arrhenius Eq:

$$k(T) = A\,exp\left(\frac{-E_a}{R\,T}\right) \tag{3}$$

where A is the preexponential factor, E_a is the activation energy, R is the gas constant (8.314 J.mol^{-1}.K^{-1}).

For constant heating rate, $\beta = \frac{dT}{dt}$, Eq (1) can be rearranged as:

$$\beta \frac{d\alpha}{dT} = A\, exp\left(\frac{-E_a}{R\,T}\right) f(\alpha) \qquad\qquad (4)$$

1.2 Methods to determine the activation energy independently of the kinetic model

Different approaches have been proposed to calculate the kinetic parameters, A and E_a, without assuming any reaction model. Isoconversional or model free methods have also been used to process TGA data and obtain the activation energy without an explicit model from experimental thermal degradation data. Among the more prominent methods in this category are the Friedman method (Friedman, 1964), Kissinger (Kissinger, 1957) and Ozawa-Flynn-Wall (Ozawa, 1965) allowing the determination of the activation energy from dynamic experimental data measured at different heating rates (Jain, Mehra, & Ranade, 2015).

1.2.1 Isoconversional Ozawa-Flynn-Wall method

The isoconversional method of Ozawa-Flynn-Wall (OFW) (Ozawa, 1965), (Flynn & Wall, 1966), which uses the Doyle approximation (Doyle, 1962), is a method which assumes that the conversion function $f(\alpha)$ does not depend on the heating program. In this model the activation energy is a function of the degree of conversion and can be obtained from the slope of the linear relationship between $\ln(\beta)$ and 1/T given by the Eq:

$$ln(\beta) = const - 1.052 \frac{E_a}{RT} \qquad\qquad (5)$$

This method makes it possible to determine the activation energy without previous knowledge of the kinetic model. If the calculated values of E_a were the same for all the values of α, the existence of a single step reaction could be concluded. On the other hand, a change of E_a with the degree of conversion would be an indication of a complex reaction mechanism that invalidates the separation of the variables involved in the OFW analysis (de Britto & Campana-Filho, 2007), (Vyazovkin et al., 2011).

1.2.2 Kissinger's method

The Kissinger method (Kissinger, 1957) is used to determine the activation energy from plots of the logarithm of the heating rate *versus* inverse of

temperature at the maximum reaction rate, in constant heating rate experiments. The activation energy is obtained from the slope of the straight line according to the Eq:

$$\ln\left(\frac{\beta}{T_p^2}\right) = \frac{\ln(AE_a)}{T} + \ln\left[n(1-\alpha_p)^n\right] - \frac{E_a}{RT_p} \qquad (6)$$

where T_p and α_p are the absolute temperature and the degree of conversion respectively, at the maximum weight loss rate. As in the OFW method, in the Kissinger method the activation energy can be determined without a precise knowledge of the reaction mechanism. However, it should be taken into account that the activation energy obtained by this method is only reliable if $f(\alpha_m)$ is independent of the heating rate β (Vyazovkin et al., 2011).

There are several works in the literature reporting on the calculation of the activation energy (E_a) of the thermal decomposition of chitosan and its derivatives. Nevertheless, the different experimental conditions in each work, isothermal or dynamic conditions, in air or in a nitrogen atmosphere, as well as different DDs, make it very difficult to compare the different results.

Wanjun et. *al* (Wanjun et al., 2005) studied the thermal degradation of chitin (DD=7.5%) and chitosan (DD= 85%) by using TGA and DSC in a nitrogen atmosphere. By applying the Friedman method they studied the dependence of the activation energy on the degree of conversion and found no variation in the case of chitin, while activation energy increased with the degree of conversion in the case of chitosan. This suggests different degradation mechanisms for acetylated side chains that increase the thermal stability of the linked main chain parts. De Britto and Campana-Filho (de Britto & Campana-Filho, 2007) performed dynamic and isothermal experiments for chitosan with DD=88% and reported that the activation energy was E_a=149,6 KJ/mol and E_a=138,5 kJ/mol applying the Ozawa-Flynn-Wall and Kissinger method, respectively. E_a=153 kJ/mol were obtained in isothermal conditions. They also found that the kinetic model that best fitted the experimental data was the catalytic Sestak-Berggren model.

1.3 Reaction models

Different kinetic models, $f(\alpha)$, have been proposed in the literature, to simulate thermal degradation of chitosan The most common equation model for decelerating-type processes is a reaction-order model where n is the reaction order:

$$f(\alpha) = (1 - \alpha)^n \tag{7}$$

Sestak-Berggren (Šesták & Berggren, 1971) includes the consideration of different mechanisms in the empirical model depending on three parameters m, n, and p:

$$f(\alpha) = \alpha^m (1 - \alpha)^n - [ln(1 - \alpha)]^p \tag{8}$$

This is normally used in its reduced form (p=0), which represents an example of the autocatalytic model.

1.4 Curve fitting

Numerical calculation allows fitting non-isothermal degradation thermograms to empirical models using non-linear least squares search routines. In this work, modelling of a TGA heating ramp was performed by substituting the heating ramp by a series of successive 0.5 ºC temperature steps, followed by isothermal periods Δt_i, to obtain the average experimental heating rate. After each isothermal stage i, at temperature T_i, with the conversion degree α_i, a sudden change of temperature to T_{i+1} was considered to maintain the conversion degree unchanged, $\alpha_{i+1,0}=\alpha_i$. The conversion degree at the end of the i+1 isothermal was determined by an iterative procedure. The rate of change of the conversion degree was calculated using Eq (1), and the conversion degree at the end of the i+1 isothermal was determined as a first approximation by integration of Eq (1) to obtain the value $\alpha_{i+1,1}$. The mean value of $\alpha_{i+1,1}$ and $\alpha_{i+1,0}$ was used to recalculate dα/dt, and with this derivative a new value of the conversion degree at the end of the step was calculated. A convergence of the value of α_{i+1} was obtained after three iteration cycles. This procedure can determine the thermogram for a given kinetic model corresponding to Eq (1) with given values of the model parameters. The thermograms predicted in case of superposition of more than one degradation mode are also readily obtained. The model parameters were determined by simultaneous fitting of the conversion degree and the weight derivative thermograms at a heating rate of 20 K/min.

2 Materials and methods

2.1 Materials

Chitosan medical grade polymer was purchased from Novamatrix (PROTASAN UP 80/20) with DDs between 80-89% and apparent viscosity 20-199 mPa s. Acetic acid (99%), Sodium hydroxide, acetic anhydride, deuterium oxide (99%) and deuterium chloride (99%) were purchased from Sigma-Aldrich.

2.2 N-Acetylation of chitosan

Chitosan medical grade was dissolved in 20 ml acid acetic 2 % (w/w) by stirring for three hours, then 15 ml of methanol were added, and the solution was stirred overnight. Different quantities of acetic anhydride were mixed with methanol and added to the chitosan solution. The reaction was stirred overnight and then NaOH 1M was added until neutral pH. The entire process was carried out at room temperature. Finally the N-acetylated chitosan was freeze-dried to obtain a white powder.

2.3 ^{1}H-NMR Spectroscopy

The DD of the chitosan samples was evaluated by proton nuclear magnetic resonance (^{1}H-NMR). The spectra were recorded between 0-10 ppm in a Varian Unity plus 300 at 70ºC(Fernandez-Megia, Novoa-Carballal, Quiñoá, & Riguera, 2005). Chitosan powder (5 mg /mL) at different DDs was dissolved in a deuterated aqueous acid (D_2O/ DCl) (Hirano et al., 1976). The chitosan solutions were dissolved by stirring at $70^{\circ}C$ for 1 h. The DD was calculated by the integrals of the peak of proton H1 of deacetylated monomer (H1D) and the peak of the three protons of acetyl group (H-Ac) (Lavertu et al., 2003):

$$DD(\%) = \left(\frac{H1D}{H1D + {HAc}/{3}} \right) 100 \qquad (10)$$

2.4 Thermogravimetric analysis (TGA)

Thermogravimetric measurements were performed using a TA-Instrument SDT-Q600 system. TGA tests were carried out in alumina crucibles in which samples with a weight between 5 and 10 mg were heated from 300 to 1073 K at different heating rates ranging from 10 K/min to 40 K/min. TGA experiments were performed under a nitrogen atmosphere (flow 20 ml/min).

3 Results and discussion

3.1 Deacetylation degree

The DD of chitosan powder obtained from the N–acetylation reaction was calculated using the ^{1}H-NMR spectroscopy by applying Eq (10), being 85% for the original chitosan and 72%, 64%, 59% and 50% for the N-acetylated samples. Samples were identified according to their DD: CHT-72, CHT-64, CHT-59 and CHT-50 except the original chitosan CHT-Or.

3.2 Thermogravimetric analysis

The thermal degradation of CHT-Or and N-acetylated samples, CHT-72, CHT-64, CHT-59 and CHT-50, were analyzed in detail with dynamical TGA experiments at different heating rates ranging from 10 K/min to 40 K/min. Four phenomena were observed (Figure S1): between room temperature and 400 K the weight loss is due to the evaporation of the absorbed water, between 500 and 800 K two overlapped peaks in the weight derivative are due to the degradation of the polymer chains as explained below, then a slow and continuous weight decrease follows until the end of the thermogram at 1000 K. To isolate the two central processes a baseline was drawn between 500 and 800 K in the weight derivative curve. The integration of the weight derivative peak in this region allows calculating the conversion degree, which is thus equal to 0 at 500 K and equal to 1 at 800 K, as shown in Figure 1a and Figure 1c.

Figure 1a shows the experimental conversion curves for the thermal degradation of CHT-Or, at different heating rates, between 500 and 800 K. We excluded in this work the first degradation stage, below 273 K corresponding to the water loss. It can be observed that when the heating rate (β) increases, the curves shift towards higher temperatures. This effect is better observed in the derivative DTG curves, Figure 1b, where the maximum of the derivative of the conversion degree appears at: 576 K, 583 K, 591 K and 596 K for heating rates: 10 K/min, 20 K/min, 30 K /min and 40 K/min, respectively.

Figure 1. Conversion degree (a) and its derivative (b) of original chitosan (CHT-Or) at different heating rates. Conversion degree (c) and its derivative (d) of chitosan with different DD at 10 K/min.

Figure 1c shows the conversion degree for chitosan and its acetylated derivatives, at a heating rate of 10 K/min and Figure 1d shows its derivative. It can be observed that whereas the main peak remained at a temperature around 570 K for all samples, a second phenomenon (appearing as a shoulder on the

high temperature side of the main peak between 600 and 650 K) increased in intensity as DD decreased.

According to (Guinesi & Cavalheiro, 2006), (Nam et al., 2010), the first degradation stage, around 550-600 K, is attributed to the depolymerization of chitosan D-Glucosamine (Glc) units, while the second decomposition temperature can be ascribed to the degradation of N-Acetyl-D glucosamine (GlcNAc). At temperatures above 750 K a slow weight loss was observed due to residual decomposition reactions produced in inert conditions. All polymer samples presented a residual mass of around 30-40%, regardless of DD, although this was not taken into consideration, as we had set the conversion degree equal to 1 at 800 K for all samples.

3.3 Determination of activation energy (E_a)

The activation energy (E_a) values were calculated following the Kissinger method (Kissinger, 1957) from the slope of the line determined by plotting $\ln(\beta/T^2p)$ against $1/Tp$, according to Eq. (6). Figure 2a shows the plots corresponding to the first degradation peak. The obtained activation energy as a function of DD is represented in Figure 2b. Although the activation energy seems to decrease with DD, there is no clear tendency. In particular in the case of CHT-72 the position of the peak measured at the lowest heating rate gives a quite low and unrealistic activation energy for this sample. The results show a greater activation energy corresponding to the second peak at higher temperatures. This method has some limitations, as has been pointed out in the study presented by the International Confederation for Thermal Analysis and Calorimetry (ITAC) (Vyazovkin et al., 2011). A strict linear relationship is only accomplished for a first order kinetic model. Another important limitation of this method is that it can only be adequately applied to single-step kinetics. In the case of multi-step kinetics, as in our case, it would be necessary to use an isoconversional method to better estimate the activation energy.

Figure 2. Kissinger plot of $\ln\beta/Tp$ versus $1000/Tp$ for the chitosan and its N-acetylated derivatives (a); E_a values obtained from the slope of the straight lines (b).

To apply the isoconversional OFW method to the thermal degradation of chitosan scanned at different heating rates, curves of $\ln(\beta)$ versus $1000/T$ were plotted for experimental data in the range $0.05<\alpha<0.95$ (see Figure 3 for CHT-Or; the rest of

the polymers presented similar representations). It can be observed that, in general, the experimental points were quite well aligned, with the correlation coefficient ρ^2 ranging between 0.94 and 0.9994. For the rest of the polymers, experimental points were well aligned, with $\rho^2 > 0.9$, except for the highest conversion degree $\alpha = 0.95$ with a ρ^2 as low as 0.33 for CHT-59.

Figure 3. Representation of the ln β as a function of the inverse of temperature (1000/T) calculated for different values of the degree of conversion, α for CHT-Or sample. The linear plot is also represented for each α value.

The activation energy as a function of the degree of conversion was determined by applying Eq. (5) to the slope of these straight lines. The results of the activation energy for each sample as a function of the degree of conversion in the range $0.05 < \alpha < 0.90$ are represented in Figure 4. In the region $0.15 < \alpha < 0.7$ the activation energy values ranged between 150 and 250 kJ/mol with no clear dependence on DD. In all cases small changes with the degree of conversion were observed with a net increase for all samples, of around 50 kJ/mol. In the region corresponding to higher degrees of conversion, $0.7 < \alpha < 0.95$, the values of E_a differ for each chitosan derivative. While CHT-Or and CHT-72 showed a decrease in activation energy, the rest of the samples showed an increase. This was particularly pronounced in the CHT-64 sample.

It is worth noting that no discontinuities can be observed in the Ea vs α plot of Figure 4 in any of the samples that could evidence the preponderance of the high-temperature degradation stage. Thus it is difficult to reach any conclusion on the activation energy of this high-temperature process using OFW method. This fact reveals that even at high conversion degrees both degradation mechanisms are highly overlapped. Anyway, in order to emphasize the different features found with curve fitting procedure, the results of the average Ea for different conversion degree regions are listed in Table 1. In all cases the average Ea is higher for the interval corresponding to higher values of the degree of conversion. The increase of Ea with the conversion degree has previously been found by Wajun et al. (Wanjun et al., 2005) by applying the Friedman method for chitosan at DD=85%. In our results this dependence was most noticeable when DD was lowest, CHT-64 being the sample with the highest variation. It is worth noting that Wanjun et al. found no dependence of E_a on α for chitin, although, as they explained, the presence of randomly acetylated side-chains confers stability on the polymer.

Figure 4. Activation energy as a function of the conversion degree, α, for all samples.

Table 1.- Activation energy as obtained from the Kissinger method and the average obtained from the OFW method. The average has been calculated for different conversion degree regions: all values (0.1<α<0.95), low conversion degree (0.1<α<0.6) and high conversion degree (0.6<α<0.95); error is calculated as the standard deviation.

3.4 Kinetic model

Once the values of the activation energy for the main degradation process have been obtained from isoconversional model-free methods, it is possible to test the prediction of the different kinetic models. The shape of the conversion degree and its temperature derivative were reproduced for the thermograms obtained at a heating rate of 20 K/min. Two overlapped degradation processes were considered. In the first fitting the activation energies were kept constant with the values obtained from the OFW method, while the remaining parameters were determined by the least squares search routine. In the case of CHT-Or, in which the high temperature degradation peak is small, first order kinetic model (Eq (1), (3) and (7)) predicted a quite asymmetric peak in dα/dT qualitatively different from the experimental curves (results not shown). With second order kinetics the peak obtained was broader than the experimental for any value of the preexponential factor A, which is the only adjustable parameter since in this case E_a is kept constant in the search routine (Figure 5a).

Figure 5. Experimental and fitted data for the derivative of the conversion degree (a) for CHT-Or at 20 K/min, and (b) for CHT-50 at 20 K/min, (□ Experimental, — Sestak-Berggren fitting curve, …Sestak-Berggren and --- Second order). The fitted computational Sestak-Berggren curve is superimposed on the experimental data. Fitting parameters are shown in Table 2.

Better results were obtained when the Sestak-Berggren model (Eq (1), (3) and (8)) was applied using the activation energies obtained by the OFW method. In this case the experimental curve is reproduced quite accurately. However, much better results were obtained when the computational method was applied, assuming a Sestak-Berggren reaction model and searching for the activation energy and preexponential factor. The optimized values of A and E_a are shown in Table 2. The fit of the experimental results is then very good, but the values of the preexponential factors for both degradation processes seem unrealistic. The value of the activation energy of 190 kJ/mol is required to get a narrow peak in dα/dT.

The same procedure was followed for the CHT-50 sample. In this case it was interesting to check whether the different models were able to reproduce the high temperature degradation stage that appeared as a shoulder in the derivative curve. Figure 5b shows the results of the different fitting methods compared with the experimental data. It can be seen that in this case the Sestak-Berggren model predicts a sharper separation of the two degradation processes in the dα/dT. Second order kinetics still draws a broader main peak, and perhaps because of this the overlapping region of the two processes is more similar to the experimental thermogram.

Table 2.- Pre-exponential factor and activation energy used to reproduce the model curves presented at Figure 5 for fitting of the experimental data of CHT-Or at 20 K/min and CHT-50 at 20 K/min.

Thus, Sestak-Berggren reaction model was selected for a detailed analysis of the shape of the TGA thermograms. Two main features can be noted in the dependence of the shape of the dα/dT, traces shown Figure 1d, with the deacetylation degree. On the one hand, as already mentioned above, the increase of the strength of the high-temperature peak with decreasing DD. On the other hand the width of the main, low-temperature peak, becomes narrower in CHT-72 and CHT-64 than for DD higher or lower DD values. This feature was confirmed in the thermograms recorded at the different heating rates. Fitting to the kinetic model reveals that the width of the dα/dT peak is mainly determined by the activation energy since a higher value of E_a determines a faster increase of the degradation rate with increasing temperature and thus the weight loss takes place in a narrower temperature interval. The parameters n and m were less influent and could be fixed with the average values found by a preliminary search routine conducted in all the samples: n=2 and m=0.4. It can be said that in this way Sestak-Berggren model equations are as modified second order reaction model (in which m=0). Quite good fits to the experimental results were obtained in all the samples. Figure 6 shows the case of CHT-50 while the comparison between model and experimental traces in the rest of samples are shown in Figures S2a to S2c in the supplementary data. In these figures, the model calculated curves for each degradation process is represented. Please note that the high temperature degradation stage takes place in a quite broad temperature interval. The values of A, E_a and the weight fraction assigned to each degradation stage were obtained by the least squares fitting and are listed in Table 2. The

weight fraction assigned by the model calculation to each degradation process is in good agreement with the value of DD.

Figure 6. Experimental and fitted data of the derivative of the conversional degree for CHT-50 at 20 K/min, considering two peaks (□ Experimental, — Sestak-Berggren fitting curve, — Peak 1 and — Peak 2).The fitted curve is superimposed to the experimental data. The contribution of each peak is also shown.

As expected, the activation energy of the low-temperature peak is higher in CHT 72 and CHT 64 than in the other samples with lower or higher content of deacetylated units. This feature shows the coupling of the degradation mechanism involved in the deacetylated monomeric units with the presence of acetylated ones, i.e., that the changes in the width of the $d\alpha/dT$ peak is not produced only by the overlapping of the two degradation peaks but is due to an influence of the presence of acetylated units in the copolymer chain. On the other hand, curve fitting provides a consistent value of the activation energy of the high-temperature process with a value between 100 and 140 kJ/mol slightly increasing with decreasing DD. The low value of E_a for the high-temperature process can be also considered as an indication of the mutual influence between the two degradation processes taking place in the copolymer chain since the cleavage of the deacetylated monomeric units can induce the loss of adjacent acetylated units

5. Conclusions

The thermal stability of chitosan of varying DD was analyzed in dynamic experiments with heating rates ranging from 10 to 40K/min. While the main peak remained at approximately the same temperature for all samples, a second degradation process appears as a shoulder in the high temperature side of the main peak, increasing in intensity as the DD of the sample decreased.

Computer simulation of the experimental thermograms obtained by curve fitting of Sestak-Berggren model allows determining that the fraction of the weight loss in the low-temperature degradation process agrees with the deacetylation degree of the sample. Thus supporting that low-temperature peak is due to thermal degradation of deacetylated units. Model fitting allows analyzing the mutual influence of both degradation processes, the activation energy of the low-degradation process significantly increases with the introduction of a fraction of

acetylated units up to around 35% and then decreases. On the other hand the activation energy of the high temperature process can be also determined showing a value that slightly increases with an increase of the fraction of acetylated units. The calculation of the activation energy using methods independent of the kinetic model did not reveal these features due to the superposition of the two processes in the same temperature interval.

Acknowledgements

References

Sestak, J., & Berggren, G. (1971). Study of the kinetics of the mechanism of solid-state reactions at increasing temperatures. *Thermochimica Acta*, *3*(1), 1–12.

Bai, F., Guo, W., Lü, X., Liu, Y., Guo, M., Li, Q., & Sun, Y. (2015). Kinetic study on the pyrolysis behavior of Huadian oil shale via non-isothermal thermogravimetric data. *Fuel*, *146*(January), 111–118. http://doi.org/10.1016/j.fuel.2014.12.073

de Britto, D., & Campana-Filho, S. P. (2007). Kinetics of the thermal degradation of chitosan. *Thermochimica Acta*, *465*(1-2), 73–82. http://doi.org/10.1016/j.tca.2007.09.008

Doyle, C. D. (1962). Estimating isothermal life from thermogravimetric data. *Journal of Applied Polymer Science*, *6*(24), 639–642. http://doi.org/10.1002/app.07.v6

Flynn, J. H., & Wall, L. a. (1966). General treatment of the thermogravimetry of polymers. *Journal of Research of the National Bureau of Standards Section A: Physics and Chemistry*, *70A*(6), 487. http://doi.org/10.6028/jres.070A.043

Friedman, H. L. (1964). Kinetics of thermal degradation of char-forming plastics from thermogravimetry.

Application to a phenolic plastic. *Journal of Polymer Science Part C: Polymer Symposia*, *6*(1), 183–195. http://doi.org/10.1002/polc.5070060121

Jain, A. A., Mehra, A., & Ranade, V. V. (2015). Processing of TGA data: Analysis of isoconversional and model fitting methods. *Fuel*, *165*, 490–498. http://doi.org/10.1016/j.fuel.2015.10.042

Kissinger, H. E. (1957). Reaction kinetics in differential thermal analysis. *Analytical Chemistry*, *29*(11), 1702–1706. http://doi.org/10.1021/ac60131a045

Kumar, M. N. V. R., Muzzarelli, R. A. A., Muzzarelli, C., Sashiwa, H., Domb, A. J., M. N. V. Ravi Kumar *, †, … Dombll, A. J. (2004). Chitosan Chemistry and Pharmaceutical Perspectives. *Chem. Rev.*, *104*(12), 6017–6084. http://doi.org/10.1021/cr030441b

Muzzarelli, R. A. A. (2009). Chitins and chitosans for the repair of wounded skin, nerve, cartilage and bone. *Carbohydrate Polymers*, *76*(2), 167–182. http://doi.org/10.1016/j.carbpol.2008.11.002

Ozawa, T. (1965). A New Method of Analyzing Thermogravimetric Data. *Bulletin of the Chemical Society of Japan*, *38*(11), 1881–1886. http://doi.org/10.1246/bcsj.38.1881

Peluso, G., Petillo, O., Ranieri, M., Santin, M., Ambrosic, L., Calabró, D., … Balsamo, G. (1994). Chitosan-mediated stimulation of macrophage function. *Biomaterials*, *15*(15), 1215–1220.

Taboada, E., Cabrera, G., Jimenez, R., & Cardenas, G. (2009). A kinetic study of the thermal degradation of chitosan-metal complexes. *Journal of Applied Polymer Science*, *114*(4), 2043–2052. http://doi.org/10.1002/app.30796

Vyazovkin, S., Burnham, A. K., Criado, J. M., Pérez-Maqueda, L. a., Popescu, C., & Sbirrazzuoli, N. (2011). ICTAC Kinetics Committee recommendations for performing kinetic computations on thermal analysis data. *Thermochimica Acta*, *520*(1-2), 1–19. http://doi.org/10.1016/j.tca.2011.03.034

Wanjun, T., Cunxin, W., & Donghua, C. (2005). Kinetic studies on the pyrolysis of chitin and chitosan. *Polymer Degradation and Stability*, *87*(3), 389–394. http://doi.org/10.1016/j.polymdegradstab.2004.08.006

Fernandez-Megia, Eduardo, Novoa-Carballal, Ramón, Quiñoá, Emilio, & Riguera, Ricardo. (2005). Optimal routine conditions for the determination of the degree of acetylation of chitosan by 1H-NMR. Carbohydrate Polymers, 61(2), 155-161. doi: http://dx.doi.org/10.1016/j.carbpol.2005.04.006

Hirano, Shigehiro, Ohe, Yasuo, & Ono, Haruhiro. (1976). Selective N-acylation of chitosan. Carbohydrate Research, 47(2), 315-320. doi: http://dx.doi.org/10.1016/S0008-6215(00)84198-1

Lavertu, M., Xia, Z., Serreqi, A. N., Berrada, M., Rodrigues, A., Wang, D., . . . Gupta, Ajay. (2003). A validated 1H NMR method for the determination of the degree of deacetylation of chitosan. Journal of Pharmaceutical and Biomedical Analysis, 32(6), 1149-1158. doi: http://dx.doi.org/10.1016/S0731-7085(03)00155-9

Lim, Sang-Hoon, & Hudson, Samuel M. (2003). Review of chitosan and its derivatives as antimicrobial agents and their uses as textile chemicals. Journal of Macromolecular Science, Part C: Polymer Reviews, 43(2), 223-269.

Nam, Young Sik, Park, Won Ho, Ihm, Daewoo, & Hudson, Samuel M. (2010). Effect of the degree of deacetylation on the thermal decomposition of chitin and chitosan nanofibers. Carbohydrate Polymers, 80(1), 291-295.

Nieto, JM, Peniche-Covas, C, & Padro, G. (1991). Characterization of chitosan by pyrolysis-mass spectrometry, thermal analysis and differential scanning calorimetry. Thermochimica acta, 176, 63-68.

Pillai, C. K. S., Paul, Willi, & Sharma, Chandra P. (2009). Chitin and chitosan polymers: Chemistry, solubility and fiber formation. Progress in Polymer Science, 34(7), 641-678. doi: http://dx.doi.org/10.1016/j.progpolymsci.2009.04.001

Šesták, Jaroslav, & Berggren, Gunnar. (1971). Study of the kinetics of the mechanism of solid-state reactions at increasing temperatures. Thermochimica Acta, 3(1), 1-12.

Wanjun, Tang, Cunxin, Wang, & Donghua, Chen. (2005). Kinetic studies on the pyrolysis of chitin and chitosan. Polymer Degradation and Stability, 87(3), 389-394.
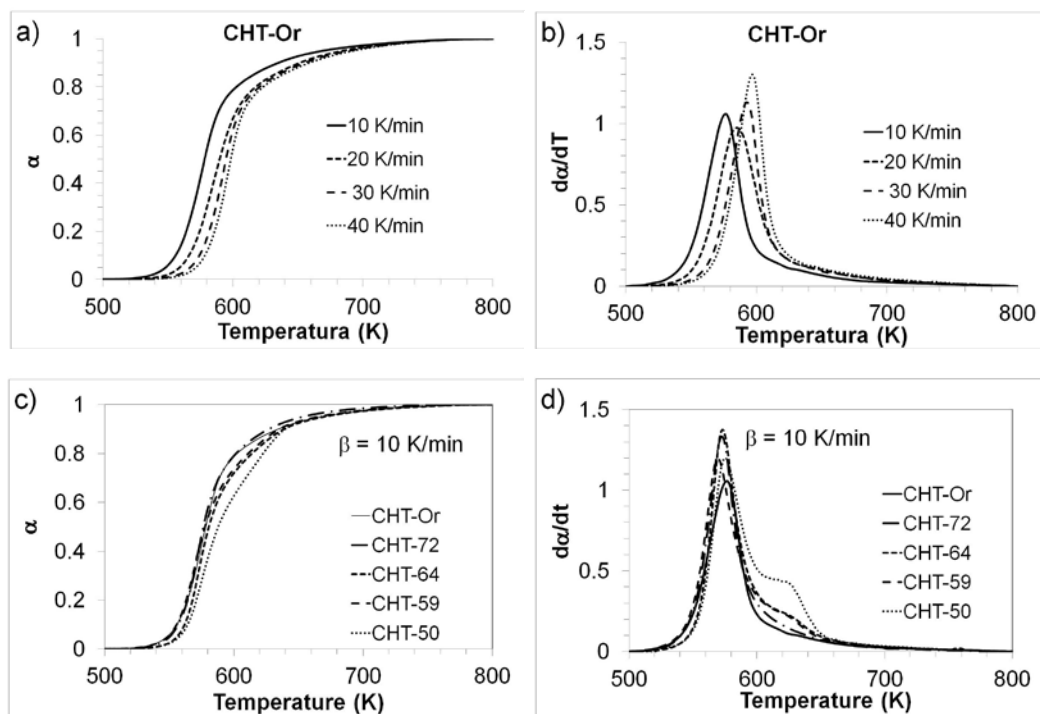
Figure 1. Conversion degree (a) and its derivative (b) of original chitosan (CHT-Or) at different heating rates. Conversion degree (c) and its derivative (d) of chitosan with different DD at 10 K/min.
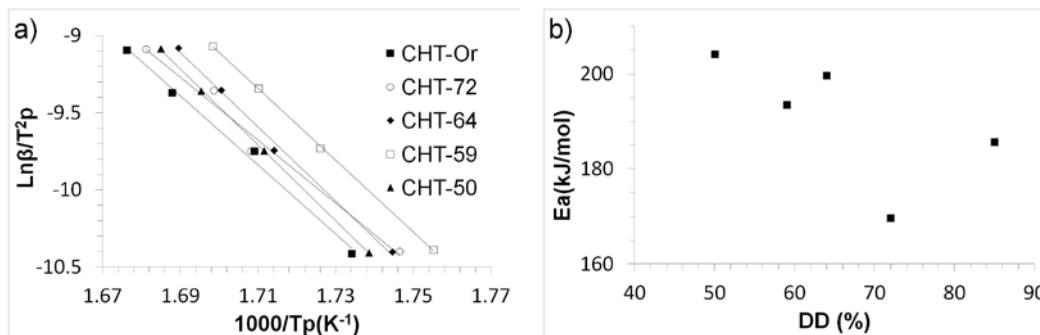

Figure 2. Kissinger plot of lnβ/Tp versus 1000/Tp for the chitosan and its N-acetylated derivatives (a); E_a values obtained from the slope of the straight lines (b).
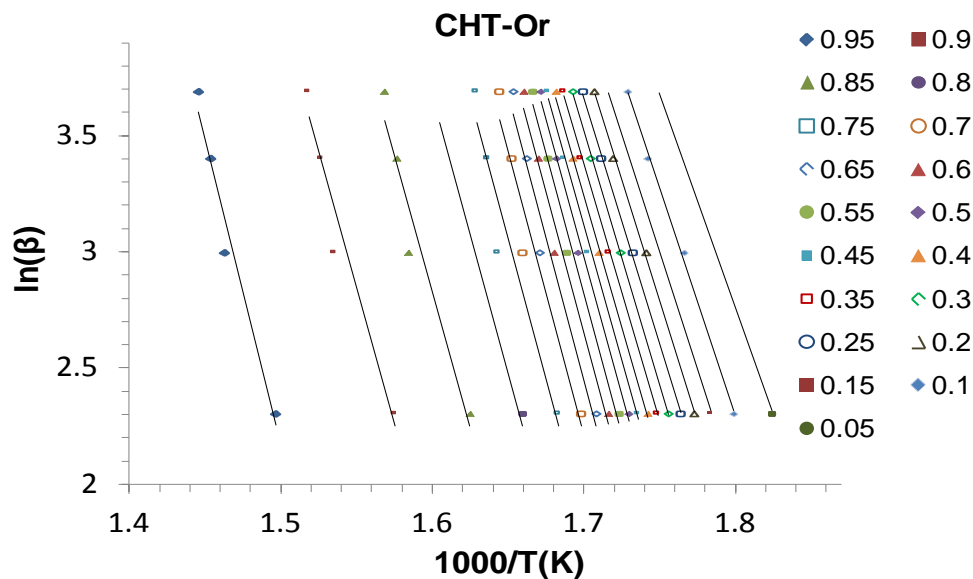
Figure 3. Representation of the ln β as a function of the inverse of temperature (1000/T) calculated for different values of the degree of conversion, α for CHT-Or sample. The linear plot is also represented for each α value.
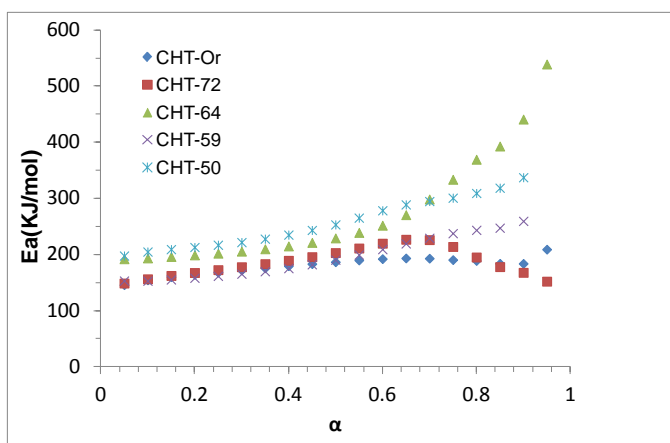

Figure 4. Activation energy as a function of the conversion degree, α, for all samples.
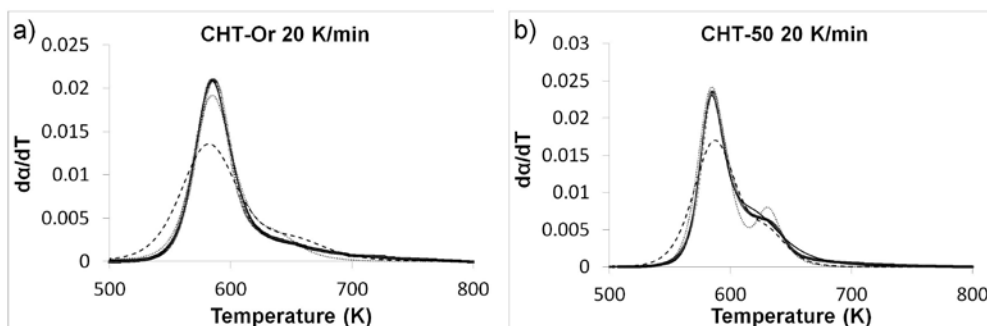

Figure 5. Experimental and fitted data for the derivative of the conversion degree (a) for CHT-Or at 20 K/min, and (b) for CHT-50 at 20 K/min, (□ Experimental, ─ Sestak-Berggren fitting curve, …Sestak-Berggren and --- Second order). The fitted computational Sestak-Berggren curve is superimposed on the experimental data. Fitting parameters are shown in Table 2.
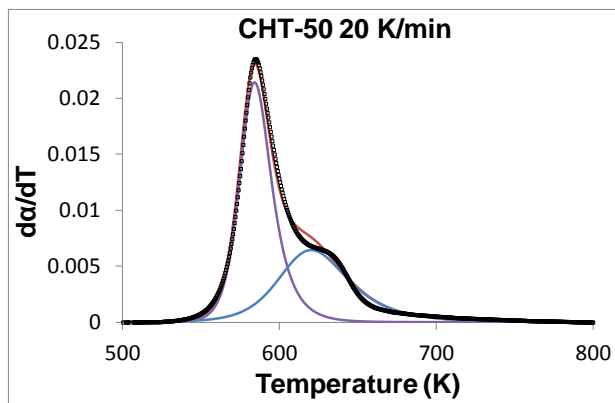
Figure 6. Experimental and fitted data of the derivative of the conversional degree for CHT-50 at 20 K/min, considering two peaks (□ Experimental,⊸ Sestak-Berggren fitting curve,– Peak 1 and – Peak 2).The fitted curve is superimposed to the experimental data. The contribution of each peak is also shown.

Table 1.- Activation energy as obtained from the Kissinger method and the average obtained from the OFW method. The average has been calculated for different conversion degree regions: all values (0.1<α<0.95), low conversion degree (0.1<α<0.6) and high conversion degree (0.6<α<0.95); error is calculated as the standard deviation.

	DD	E_a (kJ/mol)	E_a (kJ/mol) OFW		
		Kissinger	0.1<α<0.95	0.1<α<0.6	0.6<α<0.95
CHT-Or	**85**	186	179 ± 15	173 ± 14	192 ± 8
CHT-72	**72**	170	187 ± 24	182 ± 21	194 ± 27
CHT-64	**64**	200	274 ± 96	213 ± 18	378 ± 84
CHT-59	**59**	194	195 ±36	173 ± 18	239 ± 13
CHT-50	**50**	204	257 ± 42	231 ± 24	308 ± 16

Table 2.- Pre-exponential factor and activation energy used to reproduce the model curves presented at Figure 5 for fitting of the experimental data of CHT-Or at 20 K/min and CHT-50 at 20 K/min.

CHT-Or, 20 k/min				
	First stage		**Second stage**	
	A1 (s^{-1})	E_a1 (kJ/mol)	A2 (s^{-1})	E_a2 (kJ/mol)
Second order	$6 \ 10^{13}$	170	$7 \ 10^{13}$	190
Sestak-Berggren (n=2, m=0.4)	$1 \ 10^{14}$	170	$1 \ 10^{14}$	190
CHT-50, 20 k/min				
	A1 (s^{-1})	E_a1 (kJ/mol)	A2 (s^{-1})	E_a2 (kJ/mol)
Second order	$1.85 \ 10^{19}$	230	$2 \ 10^{24}$	310
Sestak-Berggren (n=2, m=0.4)	$3.6 \ 10^{19}$	230	$3 \ 10^{24}$	310
Curve fitting Sestak-Berggren (n=2, m=0.4)				
	Weight fraction (Peak 1)	**A1 (s^{-1})**	**E_a1 (kJ/mol)**	**A2 (s^{-1})**	**E_a2 (kJ/mol)**
CHT-Or	0.85	$7 \ 10^{15}$	190	$3 \ 10^{06}$	100
CHT-72	0.70	$5 \ 10^{27}$	320	$8 \ 10^{06}$	100
CHT-64	0.65	$2 \ 10^{29}$	340	$6 \ 10^{07}$	110
CHT-59	0.70	$3 \ 10^{21}$	250	$1.5 \ 10^{11}$	130
CHT-50	0.60	$3 \ 10^{23}$	270	$1.5 \ 10^{10}$	140